A Sand-Gravel Gilbert Delta Subject to Base Level Change

Chavarrías, Víctor; Blom, Astrid; Orrú, Clara; Martín-Vide, Juan Pedro; Viparelli, Enrica

DOI
10.1029/2017JF004428

Publication date
2018

Document Version
Final published version

Published in
Journal of Geophysical Research: Earth Surface

Citation (APA)
Chavarrías, V., Blom, A., Orrú, C., Martín-Vide, J. P., & Viparelli, E. (2018). A Sand-Gravel Gilbert Delta Subject to Base Level Change. *Journal of Geophysical Research: Earth Surface*, *123*(5), 1160-1179. https://doi.org/10.1029/2017JF004428

Journal of Geophysical Research: Earth Surface

RESEARCH ARTICLE
10.1029/2017JF004428

A Sand-Gravel Gilbert Delta Subject to Base Level Change

Víctor Chavarrías[1], Astrid Blom[1], Clara Orrú[1], Juan Pedro Martín-Vide[2], and Enrica Viparelli[3]

[1]Faculty of Civil Engineering and Geosciences, Delft University of Technology, Delft, The Netherlands, [2]Department of Civil Engineering, Technical University of Catalonia, Barcelona, Spain, [3]Department of Civil and Environmental Engineering, University of South Carolina, Columbia, SC, USA

Key Points:
- Sudden base level rise results in a fine signature in the foreset deposit
- Sudden base level fall results in a coarse and subsequently fine signature in the foreset deposit
- Gradual base level change is not expected to leave a signature in the deposit other than a change in elevation of the topset-foreset break

Correspondence to:
V. Chavarrías,
v.chavarriasborras@tudelft.nl

Citation:
Chavarrías, V., Blom, A., Orrú, C., Martín-Vide, J. P., & Viparelli, E. (2018). A sand-gravel Gilbert delta subject to base level change. *Journal of Geophysical Research: Earth Surface*, *123*, 1160–1179. https://doi.org/10.1029/2017JF004428

Received 13 JUL 2017
Accepted 27 APR 2018
Accepted article online 10 MAY 2018
Published online 30 MAY 2018

Abstract Laboratory experiments were conducted on a sand-gravel Gilbert delta to gain insight on its dynamics under varying base level. Base level rise results in intensified aggradation over the topset, as well as a decrease in topset slope and topset surface coarsening, the signals of which migrate in an upstream direction. Preferential deposition of coarse sediment in the topset results in a finer load at the topset-foreset break, which creates a fine signature in the foreset deposit. Base level fall has the opposite effects. Entrainment of the topset mobile armor causes a coarsening of the load at the topset-foreset break and so a coarse signature in the foreset deposit. The entrainment of the topset substrate and fine top part of the foreset may follow, which causes a fining of the load and a fine signature in the foreset deposit. The fact that the upstream sediment supply requires a certain slope and bed surface texture to be transported downstream under quasi-equilibrium conditions counteracts the effects of base level change. This information travels in the downstream direction. In nature base level change is likely so slow that the upstream sediment load maintains the topset slope and bed surface texture and so keeps the topset in a quasi-equilibrium state. Base level change is therefore not expected to leave a clear signal in a mixed-sediment Gilbert delta other than a change in elevation of the topset-foreset interface.

1. Introduction

Gilbert (1885, 1890) was the first to subdivide a deltaic deposit into three parts—the topset, the foreset, and the bottomset—where sedimentary processes are controlled by different physical processes (Figure 1). The topset deposit is formed out of layers gently inclined in the streamwise direction and deposited over the foreset by fluvial transport processes. The downstream limit of the topset is denoted as the brinkpoint. The delta foreset, or front, is dominated by avalanching processes and is formed out of steeply inclined layers that are placed over a fine-grained bottomset deposit. In general foreset layers are nearly parallel to the relatively steep delta front, and the bottomset deposit is nearly parallel to the substrate (i.e., the lake or sea bottom).

Edmonds et al. (2011) proposed to classify deltas as topset or foreset dominated. The stratigraphy of the former is mainly governed by aggradational fluvial processes on the delta top, whereas the stratigraphy of foreset dominated deltas mainly depends on avalanching processes at the delta front. They suggest that the ratio between the thickness of the topset and foreset deposits distinguishes between the two types of deltas. Gilbert deltas classify as foreset dominated deltas.

Gilbert deltas are deposited in both marine and lacustrine environments (Viparelli et al., 2012). Examples of stratigraphy created by Gilbert deltas are in the Ventimiglia valley in Italy (Breda et al., 2007, 2009), the Aguilas (Dabrio et al., 1991) and Tabernas (García-García et al., 2006) Basins in Spain, and the Kerinitis Delta in Greece (Backert et al., 2010). Peyto Lake in Canada (Smith & Jol, 1997) is an example of a modern active Gilbert delta.

The progradation of Gilbert deltas is essentially governed by two factors (Martini et al., 2017; Posamentier & Allen, 1993; Postma, 1995): (a) the influx of sediment supplied from upstream and (b) the "accommodation space," defined as the space where sediment deposits after passing the brinkpoint. Since base level variations are a main factor controlling the accommodation space, the stratigraphy of ancient Gilbert deltas has been used to reconstruct the paleo sea level (e.g., Longhitano, 2008).

The role of mixed-size sediment in Gilbert deltas is seen in the foreset deposit. Deposition of sediment downstream from the brinkpoint not only makes the delta prograde downstream but also results in the

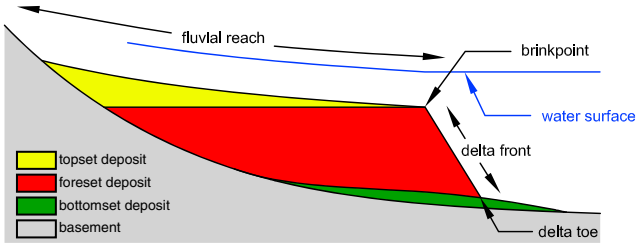

Figure 1. Stratification of a Gilbert-type delta (after Gilbert, 1890).

characteristic upward fining of the foreset deposit (e.g., Allen, 1965; Bagnold, 1941; Blom et al., 2003; Kleinhans, 2005; Postma, 1990; Van Bendegom, 1947). This is because, while avalanching downslope, (a) coarse particles roll over fines more easily than fines roll over coarse particles and (b) grain flows entrain coarse particles from a previous grain flow deposit and take them further downslope (Kleinhans, 2005).

Blom and Kleinhans (2006) developed a stratification model to describe the characteristic upward fining of the foreset deposit. They assumed that the volume fraction content varies linearly with elevation. Their stratification model was included in a numerical model of mixed-size sediment Gilbert delta progradation developed by Viparelli et al. (2012). Viparelli et al. (2014) tested the numerical model against the laboratory data obtained by Ferrer-Boix et al. (2015). The latter authors measured the size stratification in a laboratory Gilbert delta on a sloping bottomset formed during reservoir deposition due to a dam (i.e., under a constant base level). They found that as the front height increases the deposit in the lower part of the foreset becomes coarser. The numerical model has been used to predict stratigraphy under periodic base level changes (Viparelli et al., 2012). The runs indicate that slow oscillations leave a clear signature in the foreset deposit, while the stratigraphy resulting from fast oscillations approach that of a fixed base level (Howard, 1982). In particular, the signal of a slow base level rise was the formation of fine lenses in the foreset deposit (Viparelli et al., 2012). A coarsening of the bottom part of the foreset was observed during base level fall.

The objective of this study is threefold: (a) to gain insight on the progradation and size stratification of a laboratory mixed-size sediment Gilbert delta under base level rise and fall, (b) to apply and assess the Viparelli et al. (2012, 2014) mixed-size sediment Gilbert delta model under conditions of base level change, and (c) to study the effects of mixed-size sediment on a hypothetical field scale Gilbert delta whose stratigraphy is governed by grain flow processes.

The structure of the paper is as follows. Section 2 provides a description of the dynamics of Gilbert delta progradation and explains backwater effects over the fluvial reach resulting from base level change. The experimental setup and measurement techniques are presented in section 3. Section 4 deals with the laboratory results on delta migration and size stratification. In section 5 we explain the setup and the results of applying the Viparelli et al. (2012, 2014) numerical model to the laboratory experiments. In section 6 we extend the results to a hypothetical field scale Gilbert delta.

2. Background: Conceptual Dynamics of a 1-D Gilbert Delta

Deltas are three-dimensional morphological features with intricate structures such as natural levees and lobes and complex processes such as avulsions and ecological interactions (Boesch et al., 1994). In this study we focus on the effects of mixed-size sediment on delta progradation and size stratification. Therefore, we reduce the complexity of the problem retaining the essential dynamics of delta migration in one dimension. Thus, aggradational and degradational processes are averaged in the lateral direction (Paola et al., 1992). This idealized system not only provides qualitative information on deltaic processes (Lai et al., 2017; Muto & Swenson, 2005; Posamentier et al., 1992; Swenson & Muto, 2007) but also understanding of field cases, which can be well-approximated in 1-D (e.g., Ahmed & Sanchez, 2011).

The sediment that is transported over the fluvial reach is deposited downstream of the brinkpoint due to the expansion of the flow at the brinkpoint and the associated reduction in flow velocity. This deposition of sediment on the delta front makes a Gilbert delta prograde and the topset lengthen. Under conditions

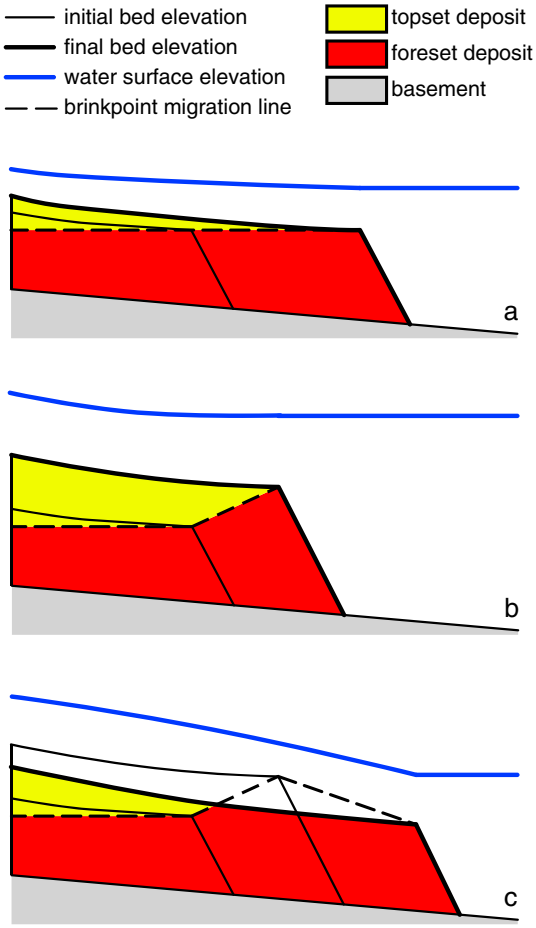

Figure 2. Schematic delta progradation under conditions of (a) a constant base level, (b) base level rise, and (c) base level rise and fall.

of a constant base level the lengthening of the topset results in topset aggradation (Gilbert, 1890; Paola et al., 2011) to maintain a slope adequate for the flow to transport the sediment load supplied from upstream. Due to the lengthening of the topset and therefore the larger volume of sediment needed to maintain the required slope, the rate at which the delta progrades decreases with time (e.g., Gilbert, 1890; Lorenzo-Trueba et al., 2009; Swenson et al., 2000).

Topset aggradation results in a streamwise decrease of the sediment load and so a streamwise reduction of the bed slope, since a smaller load requires a smaller slope to be transported downstream (Blom et al., 2016; Mackin, 1948). This results in a concave upward fluvial reach (Blom et al., 2016; Gilbert, 1890; Mackin, 1948; Sternberg, 1875). Due to the downstream decrease in bed slope, even under conditions of a constant base level, there is a streamwise increase in flow depth (Figure 2a). However, for long timescales (i.e., slow delta advance relative to the domain length) it is valid to assume that the flow is locally uniform (i.e., quasi-equilibrium conditions or quasi-normal flow (Blom et al., 2017; De Vries, 1973, 1975; Fasolato et al., 2011; Ribberink & Van der Sande, 1985)). Thus, when the base level is constant or varies slowly, fluviodeltaic morphodynamics are well approximated assuming quasi-equilibrium conditions (Ashida & Michiue, 1971; Begin et al., 1981; Culling, 1960; Martín-Vide et al., 2010; Paola, Heller et al., 1992; Ronco et al., 2010).

Under base level rise, aggradation on the topset is not only driven by delta progradation but also by the rising base level. For short timescales (i.e., fast base level changes relative to the domain length) the rising base level induces an M1 backwater (Chow, 1959) over the topset (Figure 2b). This backwater effect results in higher aggradation rates compared to the case of a constant base level, a reduction of the load arriving at the brinkpoint, and a slowdown of delta progradation. Under fast base level fall topset aggradation due to delta lengthening is counteracted by an M2 backwater (Chow, 1959) with opposite effects (faster progradation

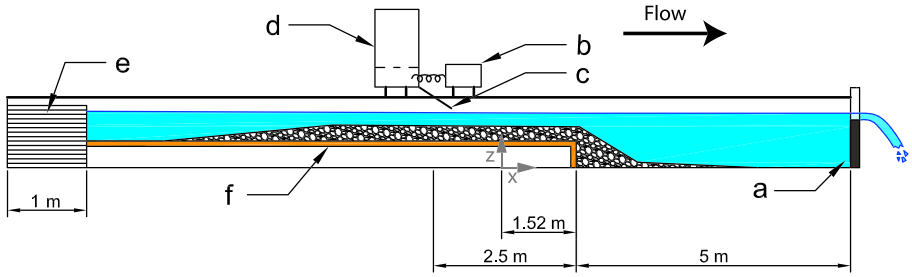

Figure 3. Not-to-scale sketch of flume and initial bed: (a) weir, (b) motor of the feeder, (c) sediment distributor plate, (d) feeder box, (e) energy dissipation and flow regulation device, and (f) wooden structure. The streamwise position *x* is defined.

and increase in load at the brinkpoint; Figure 2c). Degradation into the topset (and possibly the top part of the foreset) occurs until the slope and flow depth of the fluvial reach have adjusted to the new base level. In these conditions the brinkpoint migration line (which illustrates successive positions of the brinkpoint Swenson et al., 2000; Parker et al., 2008) is not preserved in the stratigraphic record since it does not coincide with the topset-foreset division line (which separates the topset from the foreset deposit; Figure 2c).

In this study we aim at assessing the complexities of mixed-sediment processes in the problem of a Gilbert delta subject to base level change (section 1). The first feature introduced by mixed-sediment processes is the formation of a mobile armor over the fluvial reach (e.g., Parker & Klingeman, 1982). Like the channel slope adjusts to allow for the transport of the sediment supplied from upstream (Blom et al., 2016; Gilbert, 1877; Howard, 1980; Mackin, 1948; Snow & Slingerland, 1987), under mixed-sediment conditions also the bed surface texture adjusts to allow for the transport of the coarse fractions in the sediment supplied from upstream (Blom et al., 2016; Mackin, 1948). The topset bed surface therefore coarsens compared to the substrate and forms a mobile armor.

The second feature is the fact that the larger mobility of the fines (i.e., grain size selective transport) together with the streamwise decrease in flow velocity due to delta lengthening induces preferential deposition of coarse particles in the upstream part of the topset and so downstream fining over the fluvial reach (Paola et al., 1992). This second feature reduces the mean grain size of the sediment supplied to the brinkpoint with time (i.e., a fining of the brinkpoint load (Nemec, 1990)), which has been reported also for numerical runs (Viparelli et al., 2012). This fining of the brinkpoint load reduces the topset slope near the brinkpoint, as a finer load requires a smaller slope to be transported downstream (Blom et al., 2016; Mackin, 1948). This mechanism adds to the above-mentioned reduction of the topset slope near the brinkpoint.

The third feature is the fact that the mobility of the coarse grains transported over the fluvial reach is expected to be more sensitive to base level change than the fines. This is because the transport regime of the coarse particles is generally closer to the threshold condition for significant transport.

3. Experimental Setup and Measurements

3.1. The Flume

We conduct three experiments in a tilting flume (Figure 3) in the Water Laboratory of the Faculty of Civil Engineering and Geosciences at Delft University of Technology to study the effects of base level change on Gilbert delta progradation and its size stratification. The tilting flume is 14.4 m long, 40 cm wide, and 45 cm high. An energy dissipation and flow regulation device is installed at its upstream end. At the downstream end the water surface elevation is set by a weir. Sediment is supplied to the flume with an in-house built sediment feeder.

3.2. Sediment Specifications

The parent material is a well-sorted trimodal mixture. Each sediment fraction is painted a different color to analyze the size stratification using the image analysis technique developed by Orrù et al. (2014). The geometric mean grain sizes of the fine, medium, and coarse size fractions are 1.03 mm (blue), 2.21 mm (red), and 4.42 mm (yellow), respectively (Figure 4). Appendix A provides information on the grain size definitions.

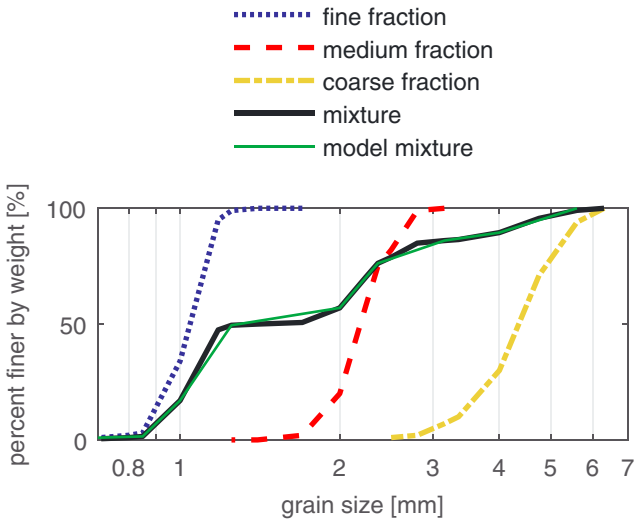

Figure 4. Grain size distributions of the fine, medium, and coarse fractions and the parent material. The model mixture (green line) is discussed in section 5.

The percentage of the fine, medium, and coarse size fractions in the parent material is, respectively, 50%, 35%, and 15%. The geometric mean grain size (d_m) of the parent material is 1.66 mm, and the geometric standard deviation (σ) is 1.75 mm. Dodecyl sulphate sodium salt is added to the sediment mixture (0.5 g/kg of sediment) to reduce the surface tension and avoid the attachment of air bubbles to the painted sediment after being released from the feeder.

3.3. Experimental Program

The initial bed consists of a mildly sloping fluvial reach (1/100) and a steep foreset (30°) that ends in a mildly sloping (1/100) basement (Figure 3). The initial deposit is built out of parent material (Figure 4). Parent material is fed at the upstream end of the test reach (Figure 3). The sediment is transported as bedload and all sediment that reaches the brinkpoint is trapped in the delta foreset.

The upstream boundary conditions (i.e., the water discharge and the sediment feed rate) are maintained constant during the experiments and are equal to 13 L/s and 280 g/min (or 1.76×10^{-6} m^3/s or 4.40×10^{-6} m^2/s), respectively. The downstream boundary condition (i.e., the base level) is kept constant in Experiment I. In Experiments II and III base level varies (Figures 5a–5c). In particular, Experiment II is characterized by base level rise (four instantaneous base level increases of 0.5 cm each), while in Experiment III we impose a stepwise sine function for rise and fall (two instantaneous base level increases of 0.5 cm each, then four falls of 0.5 cm each, and four increases of 0.5 cm each).

The duration of Experiments I–III is 14, 25, and 25.5 h, respectively. The experiments are carried out without stopping the flow to avoid start-and-stop disturbances. The imposed changes in base level are small enough to prevent the abandonment of the delta. In other words, during the entire duration of the experiments sediment is passing the brinkpoint.

3.4. Measurements

Longitudinal profiles of bed elevation and water surface elevation are measured approximately every 30 min. To this end an Ultralab UWS echosounder and a Micro-epsilon optoNCDT laser device are mounted on a carriage. Another laser device is installed at the downstream end of the flume to continuously measure the base level.

We apply the measurement technique developed by Orrù et al. (2014) to measure the size stratification of the delta deposit at the end of each experiment. The technique is based on color segmentation and provides data on the percentage of pixels of the same color in an image. As each size fraction is painted a different color, the areal fraction content covered by a color corresponds to the areal fraction content covered by a size fraction. The result is an areal fraction content rather than a volumetric one as is commonly obtained when sieving and weighting a sample. A conversion relation is applied (Parker, 1991a, 1991b) to determine the associated volumetric fraction content of a size fraction (Orrù et al., 2014).

The bed sampling procedure consists of two steps that are repeated along the entire depth of the delta once it has sufficiently dried (Orrù et al., 2014). A photo camera is installed on a movable carriage on top of the flume to take images of the entire bed surface. The second step is sediment extraction. After taking images of the entire bed surface, a 1-cm layer of sediment is removed using a wet vacuum cleaner. We then take images of the newly exposed sediment layer. These steps are repeated until the initial bed is reached. The images are cut into slices with a streamwise length of 6.25 cm (covering the entire flume width), and for each slice we determine the grain size distribution.

At the time of these experiments we were not able to measure the bed surface texture during an experiment. However, this study has encouraged us to develop a technique to measure it (Orrù, Blom, Chavarrías, et al., 2016; Orrù, Blom, Uijttewaal, et al., 2016).

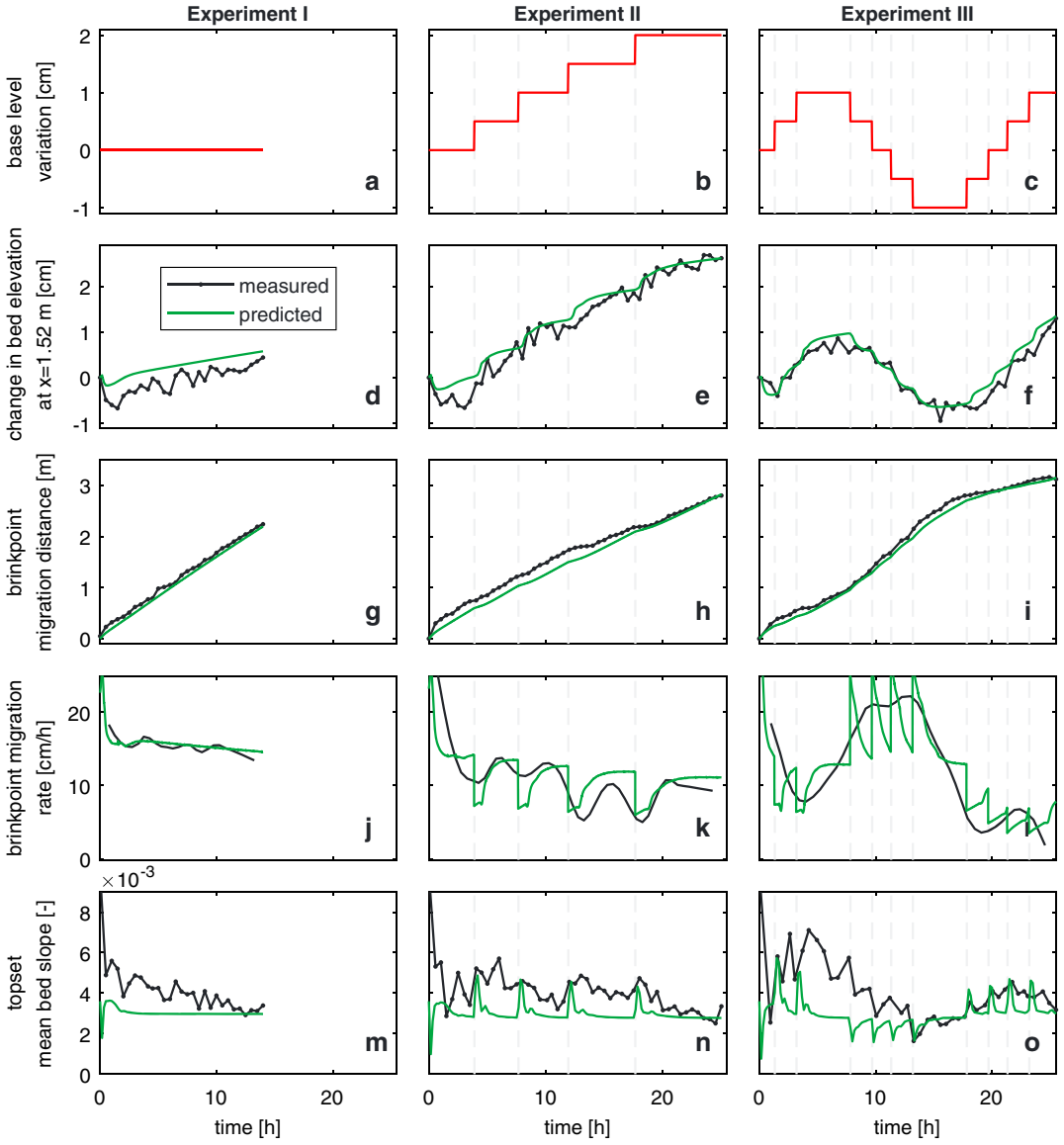

Figure 5. Characteristics of delta progradation. Subplots a–c show base level change; subplots d–f, bed elevation at the initial brinkpoint position ($x = 1.52$ m); subplots g–i, the brinkpoint migration distance; subplots j–l, the brinkpoint migration rate; and subplots m–o, the topset mean bed slope. The predicted data (green lines) are discussed in section 5.

4. Experimental Results

4.1. Delta Progradation

During the first approximately 30 min of each experiment degradation occurs (Figures 5d–5f). The beginning of each experiment is characterized by a phase of slope reduction, degradation, and development of a mobile armor on the unarmored initial deposit. After this brief degradational phase, the brinkpoint elevation follows the variation of the base level.

In all experiments the brinkpoint continues to migrate downstream, which confirms that neither delta retreat nor abandonment occurs (Muto & Steel, 1992). In Experiments I and II (constant and rising base level) the brinkpoint migration rate decreases with time (Figures 5j and 5k), as expected due to the lengthening and aggrading topset (also see section 2). Due to the base level rise in Experiment II, the brinkpoint migration rate is smaller than in Experiment I. Figure 5k reveals the presence of drops in the brinkpoint progradation rate

after every discrete rise of the base level. During the phase of base level fall in Experiment III the brinkpoint migration rate rapidly increases due to the relatively large amount of sediment deposited on the foreset, which is associated with erosion of mostly the topset deposit (Figure 5l). During the final phase of base level rise of Experiment III the brinkpoint migration rate decreases in time as sediment was trapped on the topset to restore the topset slope.

4.2. The Topset and Foreset Slopes

The backwater length scale defined as the ratio of flow depth to slope, H/S (Paola & Mohrig, 1996), is of the order of 25 m. This implies that the entire laboratory topset is located within the backwater zone induced by base level change (section 2).

At the beginning of each experiment the topset experiences a rapid adjustment phase characterized by a decrease of the mean slope as the slope that allows for transporting the parent material downstream is smaller than the imposed initial bed slope of 1/100 (Figures 5m–5o). During this initial phase a mobile armor develops to compensate for the difference in mobility between coarse and fine grains, the measurements of which will be discussed in the next section.

After this initial adjustment, the temporal change in bed slope varies from one experiment to the other. In the case of a constant base level, Experiment I, the mean bed slope very slowly decreases with time. One reason for the temporal decrease in mean topset slope is that, as the delta elongates and a larger volume of sediment is required for the topset to maintain the required slope, the bed material load at the brinkpoint decreases in time. A second reason for the steady decrease in mean topset slope may be a steady fining of the brinkpoint load (although this is not clearly observed in the measured data as will be discussed in section 4.5).

A sudden rise in base level typically causes a backwater that induces upstream migrating aggradational effects (section 2), which is associated with a decrease of the mean bed slope. However, since the entire topset of our laboratory experiments is located within the backwater zone, after each sudden base level rise the maximum rate of aggradation is observed at the upstream end of the topset, where a constant feed rate is imposed. This upstream aggradation leads to an increase of the mean topset slope. During the subsequent constant base level phase, the sediment load arriving from upstream restores the topset slope towards its quasi-equilibrium (constant base level) state (section 2).

The opposite response is observed after each sudden base level fall in Experiment III: Due to the limited flume length the maximum rate of degradation is observed at the upstream end of the topset. This degradation results in a decrease of the mean topset slope. In the subsequent phase of constant base level, the mean topset slope is slowly restored.

Figures 6a–6c confirms that the topset is concave upward (also see section 2). Aggradation due to base level rise in Experiment II has increased the absolute values of bed elevation compared to the other two experiments.

The avalanches over the delta foreset follow a two-step process (Kleinhans, 2005). Initially, sediment is deposited at the top part of the foreset forming a wedge (grain fall). When the wedge exceeds the static angle of repose, sediment moves downslope until reaching the bottom part of the foreset (grain flow). The foreset slope after the grain flow is approximately equal to the dynamic angle of repose (Kleinhans, 2005). These processes result in a foreset slope that varies between 19° and 38° with a mean value of 27°. We have not observed any significant difference between the experiments in this regard.

For our laboratory Gilbert deltas the limited length of the topset and so the upstream boundary with a constant sediment feed rate play a significant role. In section 6 we will extend these results to a field scale Gilbert delta that is characterized by a topset length that is much larger than the length of the backwater zone.

4.3. Streamwise Sorting of Topset Surface

Before we discuss the results on the stratification of the delta deposit, we consider a limited part of these results, that is, the results for the topset bed surface texture at the end of the experiments.

The geometric mean grain size of the bed surface sediment and the areal fraction content of the fine, medium, and coarse components in the bed surface sediment at the end of each experiment are presented in Figures 6d–6f and 6g–6i, respectively. The parent material is indicated for reference.

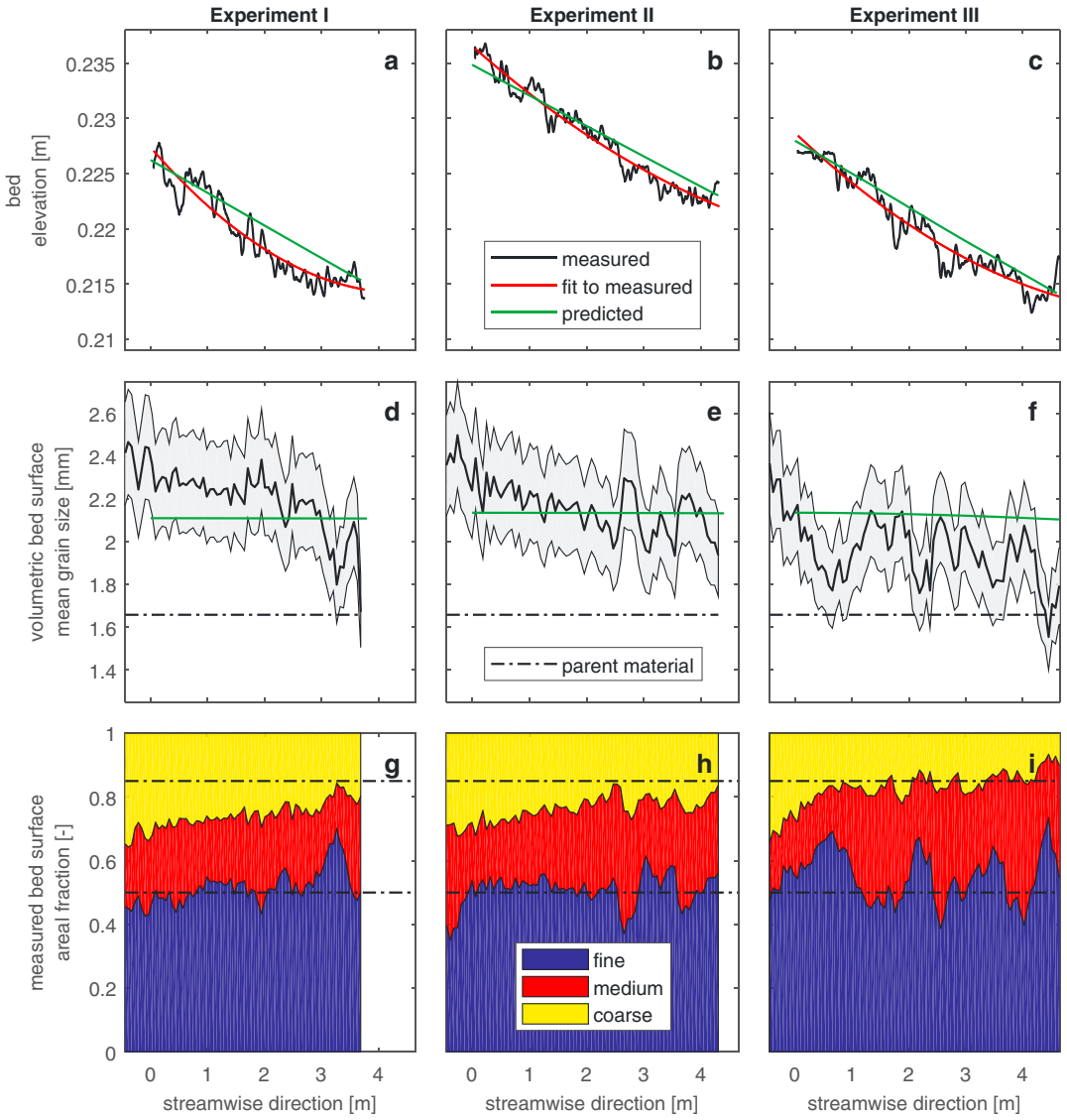

Figure 6. Bed elevation profile and surface grain size over the topset at the end of each experiment, expressed in terms of bed elevation (a–c), volumetric mean grain size of the bed surface sediment (d–f), and areal fraction content of the fine, medium, and coarse size fractions in the bed surface sediment (g–i). The dash-dotted lines indicate the parent material. The predicted data (green lines) are discussed in section 5.

During the runs a mobile armor forms to compensate for the difference in mobility between particles of different sizes, which is illustrated by the fact that in all experiments the bed surface is coarser than the parent material. A pattern of downstream fining characterizes the bed surface at the end of the experiments. Downstream fining seems to be a bit more pronounced in Experiments II and III, which are characterized by base level rise, than in Experiment I, which is characterized by a constant base level. This may underline the fact that coarse fractions are more sensitive to base level change than fines, as the mobility of the coarse fractions is closer to the threshold for significant transport.

Finally, the small scale variability in grain size distribution, in all experiments and in particular in Experiment III, is the signal of bedload sheets (Dietrich et al., 1989; Recking et al., 2009; Whiting et al., 1988). We observed that sediment was transported in low relief bedforms (two or three coarse grain sizes in height) characterized by a coarse front and a fine tail. Although we were unable to capture the dynamics of bedload sheets in detail, we did not observe differences in the geometry and grain size distribution of the bedload sheets between the experiments.

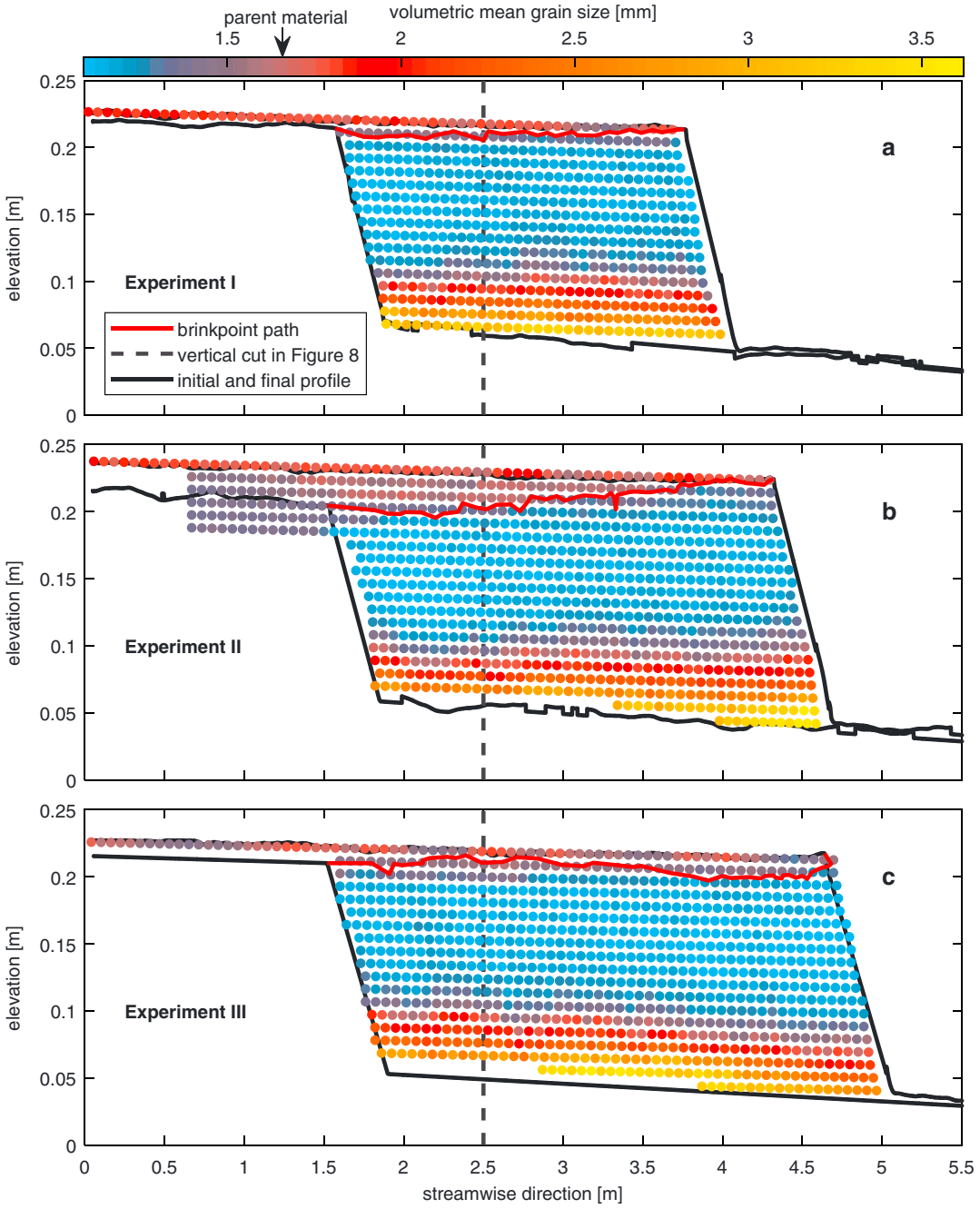

Figure 7. Stratification at the end of each experiment based on image analysis in Experiment I (a), II (b), and III (c): volumetric mean grain size over the entire delta averaged over the flume width (excluding 0.03 m near either flume wall). Both the measured initial and final bed elevation profiles are presented together with the brinkpoint path line (red). The arrow at the colorbar indicates the volumetric mean grain size of the parent material (1.66 mm). The vertical dashed line in subplot b indicates the location of the profile plotted in Figure 8.

4.4. Size Stratification of the Delta Deposit

The grain size distribution of the sediment deposited in the topset substrate (below the mobile armor) is similar to that of the sediment feed (i.e., the parent material). This is most clearly illustrated by Experiment II (Figure 7b), as in this case of ongoing base level rise the topset deposit thickness is largest.

In each experiment the deposit is characterized by the expected upward fining of the foreset deposit (also see section 2). A close look at the vertical variation in mean grain size, however, shows that the upper part of the

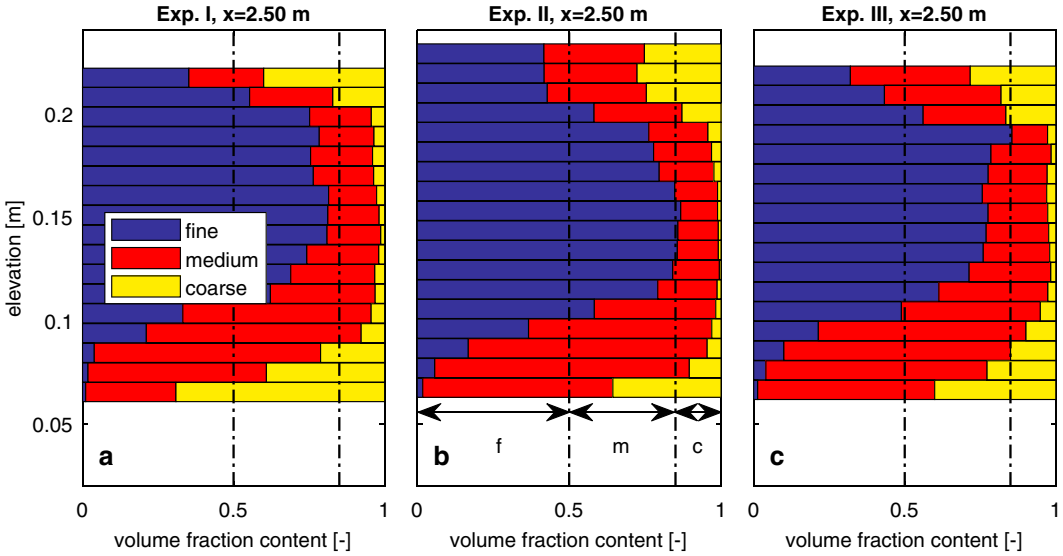

Figure 8. Vertical sorting profiles in terms of the vertical variation of the volumetric fraction content of the fine, medium, and coarse sizes in the delta deposit measured at $x = 2.50$ m in Experiments I (a), II (b), and III (c). The dash-dotted lines indicate the parent material, and "f," "m," and "c" stand for fine, medium, and coarse sediment, respectively.

foreset deposit is characterized by a nearly constant grain size distribution, while the lower part presents a clear fining upward profile (Figure 8). The strong upward fining of the lower part is in agreement with previous experimental observations (Blom et al., 2003; Ferrer-Boix et al., 2015; Kleinhans, 2005) and lee face sorting models (Blom & Kleinhans, 2006; Blom & Parker, 2004). The formation of a fine layer with nearly uniform grain size in the upper part of the foreset deposit at laboratory scale has, to our knowledge, not been observed in previous experimental work. We suspect that it is associated with the fact that our sediment mixture is well sorted and the fraction content of the fines is relatively large (50%). This contrasts with the sediment mixtures used in the above-mentioned experimental setups.

In the case of constant base level (Experiment I) a clear pattern of downstream fining or coarsening in the deposit is not observed (Figure 7a). On the other hand, the lower part of the foreset deposit of Experiment II (Figure 7b), in which the delta height increases significantly, shows downstream coarsening, which confirms the findings by Ferrer-Boix et al. (2015). This pattern may be associated with a temporal coarsening of the brinkpoint load. We will address this in more detail in the next section.

During the phase of base level fall in Experiment III the lower foreset deposit first becomes coarser in the downstream direction indicating a temporary coarsening of the brinkpoint load (compare the lower part of the foreset deposit between 3 and 3.5 m with the part between 2 and 2.5 m in Figure 7c). This is because base level fall leads to an M2 backwater over the topset and so a temporary increase of the flow velocity, and, as such, the coarser sediment of the topset surface becomes more mobile. The subsequent phase of base level fall is characterized by a temporal fining of the load, which indicates that, after entrainment of the mobile armor and the topset deposit, degradation continues into the fine top part of the foreset (compare the lower part of the foreset deposit between 4 and 4.5 m with the part between 3 and 3.5 m in Figure 7c). The part of the foreset deposit associated with the second and last cycles of base level rise is relatively short due to the rapid topset aggradation and so slow advance of the front.

4.5. Reconstruction of the Brinkpoint Load and Its Mean Grain Size

We estimate the bedload transport rate at the brinkpoint (i.e., the brinkpoint load), from the bed elevation profiles (Simons et al., 1965) assuming that the foreset porosity is equal to 0.4. The estimates are values averaged over 30 min due to our measurement frequency. In addition, the grain size distribution of the foreset and the time series of the streamwise position of the brinkpoint, respectively presented in Figures 7 and 5g–5i, allow us to roughly estimate the grain size distribution of the brinkpoint load. The grain size distribution of the brinkpoint load is computed under the assumption of a constant foreset slope equal to its average value (27°).

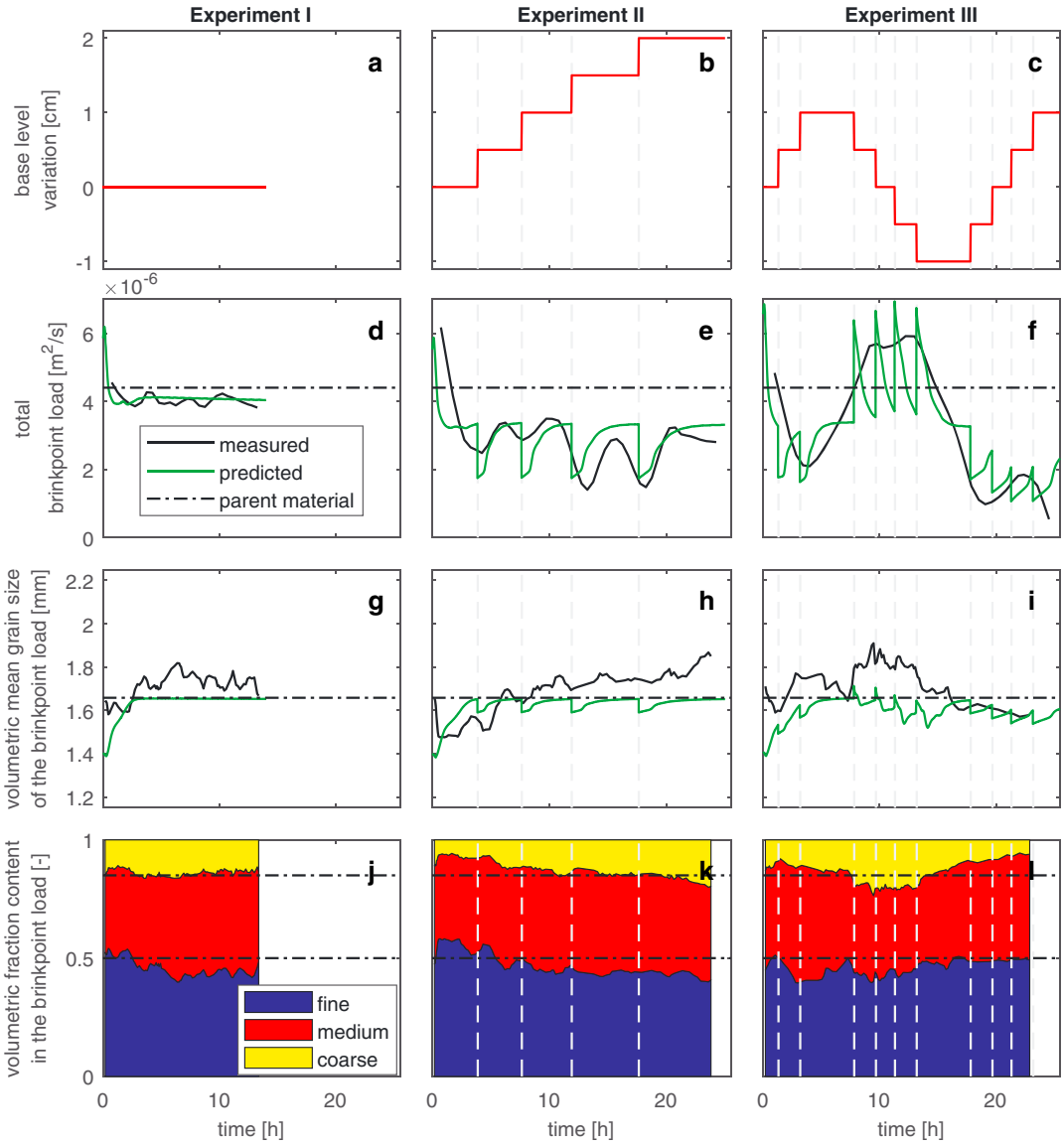

Figure 9. Characteristics of the brinkpoint load: base level change (a–c), total brinkpoint load (d–f), volumetric mean grain size of the brinkpoint load (g–i), and measured volumetric fraction content of size fraction in the brinkpoint load (j–l). The dash-dotted lines indicate the sediment feed. The predicted data (green lines) are discussed in section 5. The measured data (black lines in d–i) are based on 30-min averaged values.

In the early stage of the experiments the bedload transport rate at the brinkpoint decreases in time due to the development of a mobile armor on the topset (Figures 9d–9f). It then remains nearly constant in Experiment I, it adjusts at the moments of sudden base level rise in Experiment II, and it follows the phases of base level rise and fall in Experiment III. Under the constant base level in Experiment I, the brinkpoint load is slightly smaller than the feed rate due to the mild aggradation on the topset; under base level rise the brinkpoint load is significantly smaller than the feed rate due to the intensified topset aggradation; and during base level fall the brinkpoint load is larger than the feed rate due to degradation of the topset (and top part of the foreset).

Experiment II shows that the brinkpoint load is largely influenced by the type and rate of base level change. Despite the limited resolution of the results (due to the 30-min interval between the bed elevation measurements) we can see that a sudden base level rise induces a temporal decrease in the sediment transport rate at the brinkpoint (Figure 9e). Whether the opposite happens in Experiment III after a sudden drop of the base level is more difficult to see (Figure 9f) due to the higher frequency of base level change.

In the initial phase of the experiments the bedload at the brinkpoint coarsens due to the development of the mobile armor (Figures 9g–9i). The brinkpoint load then shows a slight temporal fining in Experiment I (Figures 9g and 9j). The fining is too mild to confirm that preferential deposition of the coarse sediment on the topset together with topset lengthening induces a temporal reduction of the mean grain size of the sediment supplied to the brinkpoint (see section 2). We note that the inferred load is slightly coarser than the fed material, which does not agree with our expectations as preferential deposition of coarse sediment would lead to a brinkpoint load that is finer than the fed sediment. At this point we have no clear explanation for this disagreement.

In Experiment II we observe how each sudden increase in base level leads to a slight fining and subsequent coarsening of the brinkpoint load (Figure 9h). Each sudden increase in flow depth causes a decrease in sediment mobility and the bedload transport rate, and the reduction of the mobility is strongest for the coarse sediment fraction. As the bed aggrades and restores the topset slope and surface texture after each sudden base level change, the mobility of the coarse fraction increases, which results in the subsequent coarsening of the brinkpoint load. The brinkpoint load coarsens with time (Figures 9h and 9k), which seems to be induced by the fact that the repeated sudden base level rise extends the time needed to form the mobile armor.

The initial rise in base level of Experiment III produces a coarsening of the load in each constant base level period, as observed in Experiment II (Figure 9i). The subsequent base level fall is characterized by an overall coarsening of the brinkpoint load associated with the entrainment of the mobile armor due to the increased flow velocity. After each sudden base level drop, the brinkpoint load first coarsens and then becomes finer during the subsequent constant base level phase. After base level fall, the finer topset substrate and the fine top part of the foreset deposit are eroded and this leads to the subsequent fining of the brinkpoint load. Finally, the last rapid base level rise is associated with a brinkpoint load that becomes slightly finer with time due to preferential deposition of coarse material on the delta topset.

5. Modeling the Laboratory Deltas

In this section we reproduce the experiments using the Viparelli et al. (2012, 2014) model of progradation of a mixed-sediment Gilbert delta under conditions of variable base level. In section 5.1 we introduce the basics of the model. The model is calibrated using the case of constant base level (section 5.2). In section 5.3 we apply the calibrated model to the cases with varying base level.

5.1. Model Characteristics

The Viparelli et al. (2012, 2014) model is composed of three submodels: (a) a delta progradation model (Kostic & Parker, 2003a, 2003b; Wright & Parker, 2005a, 2005b), (b) the Hirano (1971) model for mass conservation of each size fraction at the topset surface, and (c) a lee face sorting model describing sediment sorting over the foreset (Blom & Kleinhans, 2006; Blom & Parker, 2004).

The flow is described using the backwater equation. The upstream model boundary conditions are the water and sediment discharge and the downstream boundary condition is the base level. The flow resistance is computed using a Manning-Strickler formulation in which the nondimensional friction coefficient (C_f) is computed as

$$C_f^{-1/2} = \alpha_r \left(\frac{R_h}{k_s} \right)^{1/6} , \tag{1}$$

where $\alpha_r[-]$ is a parameter equal to 8.10 (Brownlie, 1983), $R_h[m]$ is the hydraulic radius for the bed region (Vanoni & Brooks, 1957), and $k_s[m]$ is the roughness height over a flat bed defined as

$$k_s = n_k D_{s90} , \tag{2}$$

where $D_{s90}[m]$ is the particle diameter of the bed surface such that 90% of the sediment is finer and $n_k[-]$ is a parameter within the range 1–3 (Bathurst, 1985; Ferguson, 2007; Paola, Parker, et al., 1992; Thompson & Campbell, 1979).

The active layer thickness ($L_a[m]$), which is the thickness of the topmost part of the bed that interacts with the flow and exchanges sediment with the bedload transport, is assumed proportional to the D_{s90} of the bed surface:

$$L_a = n_a D_{s90} , \quad (3)$$

where $n_a[-]$ is a parameter within the range 1–3 (Hirano, 1971; Hoey & Ferguson, 1994; Parker & Sutherland, 1990; Seminara et al., 1996). We refer to Viparelli et al. (2012, 2014) for a description of the model formulations, as well as implementation of the governing equations and the procedure for the storage of the grain size stratification.

In the simulations presented herein the grain size distribution of the parent material is discretized into eights bins: three bins for the blue fine fraction, three bins for the red medium fraction, and two bins for the yellow coarse fraction (Figure 4).

Bed degradation leads to a flux of sediment from the substrate to the active layer. The grain size distribution of the sediment transferred from the substrate to the active layer during channel degradation is equal to the grain size distribution of the topmost part of the substrate (i.e., the bed deposit below the active layer). During channel aggradation there is a flux of sediment to the substrate. The grain size distribution of the sediment transferred to the substrate is a weighted average of the grain size distribution of the active layer and that of the bedload (Hoey & Ferguson, 1994). Based on the experiments by Toro-Escobar et al. (1996) and Viparelli et al. (2010), we assume that the sediment transferred to the substrate during channel bed aggradation consists of 25% active layer sediment and 75% bedload.

The streamwise distance between computational nodes and the time step are 0.1 m and 2 s, respectively. The vertical distance between grid points for the storage of the grain size stratification is 0.01 m.

5.2. Constant Base Level Runs

We first calibrate the friction parameter n_k. To this end we compare the measured and computed longitudinal profiles of the flow depth. The value $n_k = 3.0$ provides good agreement and is in accordance with the experimental data by Meyer-Peter and Müller (1948), Gilbert (1914), and Viparelli et al. (2010).

The thickness of the active layer is related to the time needed to form the armor layer: a thin active layer allows for a quick adjustment of the surface texture. Based on the formation time of the armor in Experiment I (approximately 3 h; Figure 9g) we find that $n_a = 2.5$ is a reasonable value (section 5.1).

The sediment transport relation affects the bed surface grain size distribution and bed slope necessary to transport the sediment coming from upstream. We find that the load relation by Wilcock and Crowe (2003) provides reasonable estimates of the average slope and average grain size distribution without calibration (Figure 6), yet the predicted profile concavity and downstream fining are less pronounced than measured. This result is independent from the sediment load relation, as we found that the load relations of Meyer-Peter and Müller (1948) and Ashida and Michiue (1972) show the same behavior.

The limited profile concavity and downstream fining imply that the process of transport and deposition is not well captured by the model. According to Hoey and Ferguson (1994), the relative proportion of bedload and active layer sediment transferred to the substrate during aggradation is independent of grain size. We hypothesize that a grain size selective aggradational model for the depositional flux to the substrate may be able to capture the measured dynamics in a better way. Unfortunately, our data set cannot be used to independently assess this hypothesis since our data set on aggradational topset deposits is too small.

The comparison between the numerical and the experimental spatial variability in sediment size in the foreset deposit reveals that the vertical sorting model is not able to reproduce the two-layer structure of the foreset (Figure 10). On the other hand, the model well captures the mild decreasing progradation rate with time due to delta lengthening (Figure 5j).

5.3. Variable Base Level Runs

We have compared the experimental observations of the progradation and size stratification of Experiments II and III to the numerical predictions of the calibrated model. We find that our delta model is able to reasonably reproduce the bedload transport rates at the brinkpoint (Figures 9e and 9f), as well as the mean grain size of the brinkpoint load (Figures 9h and 9i). Predicted results are within plus and minus 10% of the measured

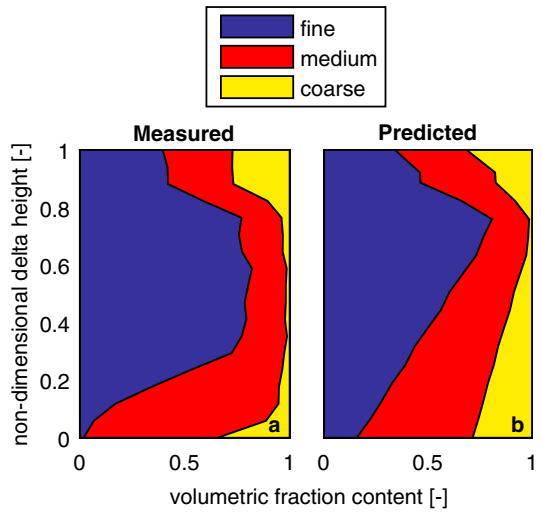

Figure 10. Measured and predicted vertical sorting profiles in terms of the vertical variation of the volumetric fraction content of the fine, medium, and coarse sizes in the delta deposit in Experiment II at $x = 2.50$ m.

values for the geometric mean size of the load. In particular, the model predicts a sudden decrease in the bedload transport rate after a sudden base level rise. This decrease is followed by a gradual increase in the transport rate until quasi-equilibrium conditions are again established and the bedload transport rate at the brinkpoint reaches a nearly constant value. A similar trend can be observed for the mean grain size of the brinkpoint load, where each sudden increase in base level corresponds to a slight temporary fining of the brinkpoint load followed by a more gradual coarsening. The model predicts changes in bedload transport rate that occur over timescales that are short compared to the measurements due to the 30-min measurement interval (section 4.5).

Just as in the calibration run, the predicted profile concavity (Figures 6b and 6c) and topset downstream fining (Figures 6e and 6f) are underestimated. However, the overall delta progradation and bed elevation changes are well captured (Figures 5e, 5f, 5h, and 5i). The sudden increase (decrease) in mean bed slope after each sudden increase (decrease) in base level due to the fact that the entire laboratory topset is located within the backwater zone is captured by the model (Figures 5n and 5o). However, the predicted change of slope is faster than the measured.

6. A Hypothetical Field-Scale Gilbert Delta Under Base Level Change

We would like to stress that the three laboratory experiments and the previous model runs focus on the mechanisms related to the progradation and size stratification of a Gilbert delta and are not an attempt to scale down a field-scale delta. The results can be used in qualitative terms (fining or coarsening, concave or convex) when analyzing a Gilbert delta in the field (Kleinhans et al., 2014; Paola et al., 2009) when grain flows are the mechanism responsible for the stratification. We here address the case of a field-scale Gilbert delta with a topset that is significantly longer than the backwater length to study how base level change affects a field-scale Gilbert delta and whether base level change is likely to leave a grain size signature in a Gilbert delta deposit.

We study the effects of a 0.5-m rise in base level using the same numerical model as that of the previous section applied to a case in which the initial topset is 5 km long. The parent material consists of two size fractions, sand and gravel (with the mean grain size of sand equal to 1mm and the one of gravel equal to 40 mm). The upstream water discharge per unit width is 2 m^2/s, and the upstream sediment load per unit width is 1×10^{-4} m^2/s. The content of gravel in the upstream sediment load is 75%. The initial bed slope and texture are such that the bed is in equilibrium with the flow rate and sediment load at the upstream end (Blom et al., 2016), which results in a slope equal to 1.872×10^{-3} and a percentage of gravel in the bed surface equal to 91.4%. The backwater length (computed as H/S) is equal to 840 m.

In a run with constant base level we see how the initial condition is in equilibrium only at the upstream end. The surface mean grain size at the upstream end of the domain does not change with time (Figure 11d). The topset lengthening causes a mild downstream fining and the associated profile concavity.

Base level rise leads to a temporal decrease of sediment mobility over the topset, the effect of which (a) increases in streamwise direction due to the M1 backwater and (b) affects the coarse grains more than the fine grains. The resulting preferential deposition of coarse grains therefore leads to a coarsening of the bed surface and the aggradation leads to a decrease of the topset slope. These signals migrate in an upstream direction but are counteracted by the mixed-size load supplied from upstream that tends to maintain the topset in a state of quasi-equilibrium in order to transport the supplied sediment downstream.

A sudden rise in base level (Figure 11b) results in a sudden and short fining of the brinkpoint load (Figure 11h), which results in a narrow fine signature in the foreset deposit. Yet for slower rates of base level change, here equal to 0.5 m over a period of 5.7 years (Figure 11c), the effect of base level rise on the brinkpoint load grain size is negligible (0.6%) compared to other natural fluctuations in the brinkpoint load such as ones due to peak flow events and migrating bars (Figure 11i). This negligible signal is because the load supplied from upstream tends to maintain the topset in a state of quasi-equilibrium and counteracts the effects of changes

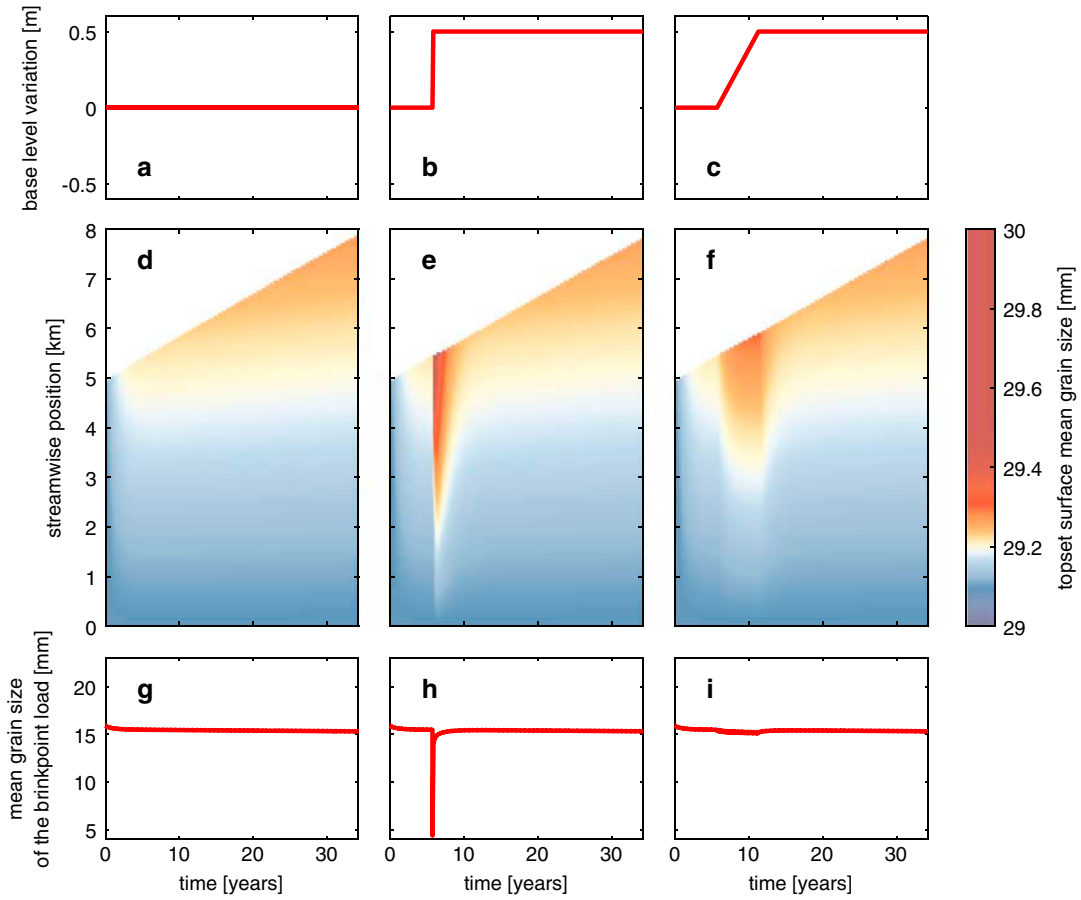

Figure 11. Predicted data for a field-scale Gilbert delta subject to base level rise: base level scenarios (a, constant; b, sudden rise; and c, gradual rise), the topset surface mean grain size (d–f), and the volumetric mean grain size of the brinkpoint load (g–i).

in base level. We therefore do not expect a clear grain size signature of base level change in the deposit of a large-scale Gilbert delta when base level changes occur over timescales of several years: The only noticeable effect of base level change on a Gilbert delta deposit likely is a change in elevation of the topset-foreset break.

The opposite case, base level fall, is illustrated in Figure 12. Sudden base level fall (center plots in Figure 12) has a number of temporary effects: a temporal increase of the flow velocity over the topset, the effect of which increases in streamwise direction due to the M2 backwater; an increased mobility of the topset surface sediment, the effect of which is largest for the coarse topset sediment; degradation of the topset armor, topset substrate, and top part of the foreset over the downstream part of the topset (the length of which depends on the backwater length); bed surface coarsening over the degrading downstream topset; an increased brinkpoint load; and an increased migration speed of the delta front. These effects are again counteracted by the sediment supply that tends to maintain the topset in a state of quasi-equilibrium and counteracts the effects of base level change by restoring the topset slope and bed surface texture.

Likewise, a gradual (vs. sudden) base level fall does not likely result in a grain size signal in the deposit of a Gilbert delta, as base level change is generally so slow that the upstream load can keep pace with the changing base level. Moreover, for a slow base level fall, the aggradation associated with front progradation may compensate the degradation due to base level fall. In this case the fine foreset deposit is not entrained.

Tectonic uplift and subsidence have not been considered in this study and they become relevant with increasing timescale. The consequences of a uniform rate of uplift or subsidence can be studied changing the reference frame and treating it as the effect of sea level fall or rise, respectively. Nonuniform subsidence occurs in deltaic environments as a result of, for instance, a co-seismic vertical displacement from large earthquakes

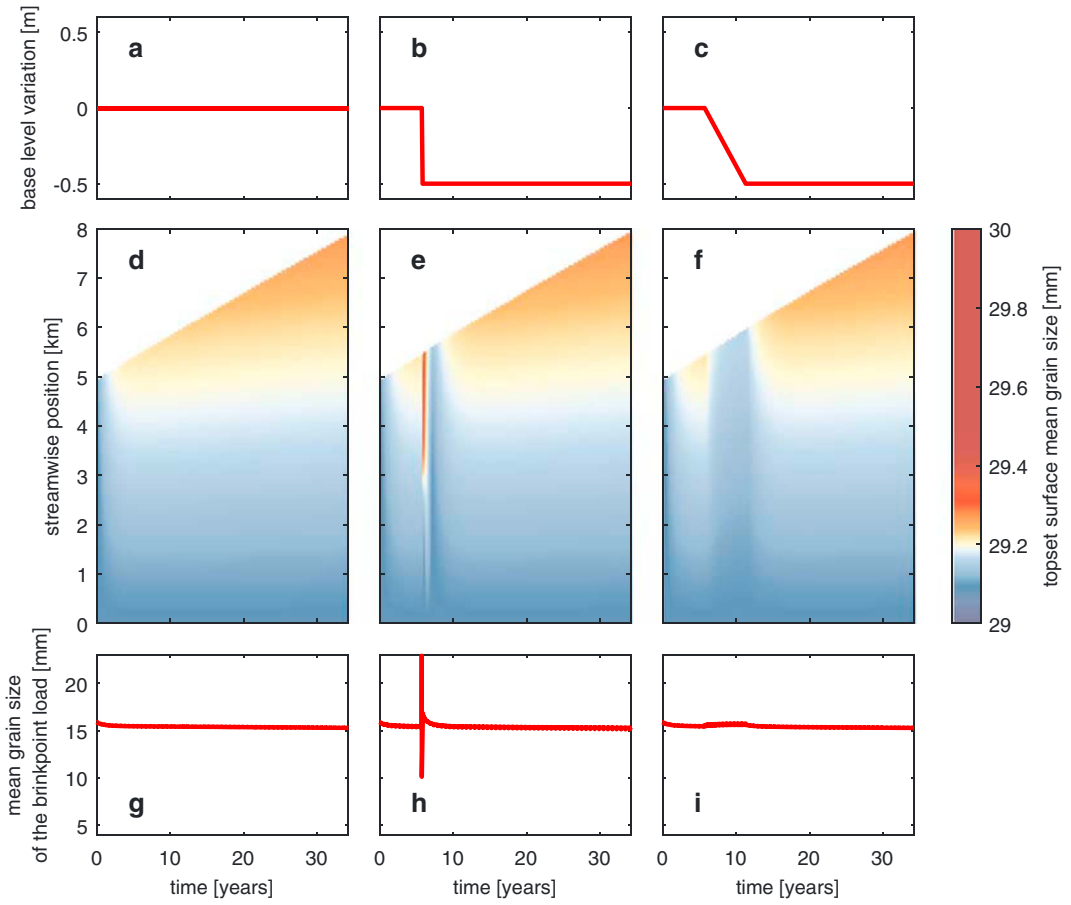

Figure 12. Predicted data for a field-scale Gilbert delta subject to base level fall: base level scenarios (a, constant; b, sudden fall; and c, gradual fall), the topset surface mean grain size (d–f), and the volumetric mean grain size of the brinkpoint load (g–i).

(Atwater, 1987). In these conditions a knickpoint in the basement occurs (e.g., Boyer et al., 2005), the consequences of which cannot be studied as a relative sea level rise. Lai et al. (2017) study delta progradation in such environments and conclude that downstream subsidence results in a shortening of the fluvial reach and a slower propagation rate.

7. Conclusions

Three laboratory experiments have been conducted to gain insight on the dynamics and size stratification of a foreset-dominated or Gilbert delta under different base level scenarios: one governed by a steady base level, one governed by base level rise, and one governed by base level variation. The sediment is transported as bedload and all sediment that reaches the brinkpoint is trapped in the delta foreset. Despite our relatively short laboratory topset we observe a concave upward profile in all experiments, which is associated with the aggradational conditions over the topset, and it is accompanied by downstream fining.

A sudden increase in base level leads to an M1 backwater over the topset. This results in a temporal decrease in the mobility of the sediment, the effect of which (a) increases with streamwise position and (b) is strongest for the coarse fraction. This results in topset aggradation, a decrease in bed slope, and a reduction of the brinkpoint load (leading to slower delta progradation) and its temporary fining, the latter creating a fine signature in the delta deposit. It also induces an aggradational and coarsening wave that migrates upstream.

Sudden base level fall leads to a situation that is almost opposite to base level rise. The resulting M2 backwater increases the flow velocity over the backwater zone of the topset. This effect increases in the streamwise direction. It creates a degradational wave that travels in an upstream direction. The brinkpoint load

temporarily increases (leading to faster delta progradation) and coarsens due to erosion of the topset mobile armor and subsequently fines due to erosion of the topset substrate and possibly the top part of the foreset, creating a coarse and subsequently a fine signature in the delta deposit.

The three laboratory experiments have been reproduced applying the Viparelli et al. (2012, 2014) numerical mixed-sediment delta model. The model captures the main mechanisms involved in progradation and size stratification of a Gilbert delta under conditions of base level change. Nevertheless the concavity and downstream fining over the topset are underestimated. We hypothesize that this is due to the submodel that sets the depositional flux of sediment to the substrate under aggradational conditions, which is grain size independent. Finally, the foreset sorting submodel, which predicts a linear increase or decrease of the content of grain size fractions over a lee face, does not capture the almost negligible upward fining in the upper part of the foreset deposit.

The effects of base level change are counteracted by the sediment supply, which tends to maintain a quasi-equilibrium topset profile in terms of slope and bed surface texture. A short fluvial reach or a slow change in base level (as typically occurs in nature) causes a fast recovery to quasi-equilibrium conditions. The consequence is that the brinkpoint load (and thus the foreset deposit) is dominated by the sediment supply. Base level change is therefore not expected to leave a clear grain size-related signal within the deposit of a sand-gravel Gilbert delta unless the vertical change is large and rapid. A change in elevation of the topset-foreset interface of a Gilbert delta likely is the best indicator of paleo base level change.

Appendix A: Definitions of Grain Size-Related Parameters

The geometric mean grain size of the fine fraction (0.8 to 1.2 mm) is 1.03 mm, that of the medium fraction (1.7 to 2.5 mm) is 2.21 mm, and that of the coarse fraction (3 to 5 mm) is 4.42 mm. The geometric mean grain size (d_m) is defined as

$$d_m = d_{ref}\, 2^{-\phi_m}\,, \tag{A1}$$

where the reference grain size d_{ref} equals 1 mm and $\phi_m[-]$ denotes the geometric mean grain size on a ϕ scale defined as

$$\phi_m = \sum_{i=1}^{N} \phi_i F_i\,, \tag{A2}$$

where N denotes the number of size fractions (here $N = 3$), $F_i[-]$ denotes the volume fraction content of size fraction i, and $\phi_i[-]$ denotes the grain size of size fraction i on a ϕ scale:

$$\phi_i = -\log_2\left(\frac{d_i}{d_{ref}}\right)\,, \tag{A3}$$

where d_i $[m]$ denotes the characteristic grain size of size fraction i. The notation with d_{ref} in equation (A3) makes ϕ_i conveniently nondimensional. The geometric standard deviation, $\sigma[m]$, is defined as

$$\sigma = d_{ref}\, 2^{\sigma_\phi} \tag{A4}$$

where $\sigma_\phi[-]$ is defined as

$$\sigma_\phi = \sqrt{\sum_{i=1}^{N} F_i\left(\phi_i - \phi_m\right)^2}\,. \tag{A5}$$

Acknowledgments
This research is supported through the Collaboration Scholarship of the Spanish Ministry of Education (2013–2014) awarded to Chavarrías and through Aspasia grant 015.007.051 of the Netherlands Organization for Scientific Research (NWO) and scholarship 10.015 of the Cornelis Lely Stichting awarded to Blom. The authors thank Erik Hendriks for setting up an earlier laboratory experiment on a mixed-sediment Gilbert delta, which helped in optimizing the setup of the current experiments. The authors wish to thank reviewers Scott Wright, Jorge Lorenzo-Trueba, and an anonymous reviewer. We also thank the Associate Editor Jon Warrick and the Editor John Buffington for their useful comments. The data used in this manuscript is registered with the DOI 10.5281/zenodo.825197 and can be downloaded from https://zenodo.org/record/825197.

References

Ahmed, K. B., & Sanchez, M. (2011). A study of the factors and processes involved in the sedimentation of Tarbela reservoir, Pakistan. *Environmental Earth Sciences*, *62*(5), 927–933. https://doi.org/10.1007/s12665-010-0578-3

Allen, J. R. L. (1965). Sedimentation to the lee of small underwater sand waves: An experimental study. *Journal of Geology*, *73*, 95–116.

Ashida, K., & Michiue, M. (1971). An investigation of river bed degradation downstream of a dam. In *Proceedings IAHR, 14th Congress* (Vol. 3, pp. 247–255).

Ashida, K., & Michiue, M. (1972). Study on hydraulic resistance and bed-load transport rate in alluvial streams. *Proceedings of the Japan Society of Civil Engineers*, *206*, 59–69. https://doi.org/10.2208/jscej1969.1972.206_59

Atwater, B. F. (1987). Evidence for great Holocene earthquakes along the outer coast of Washington State. *Science*, *236*(4804), 942–944. https://doi.org/10.1126/science.236.4804.942

Backert, M., Ford, M., & Malartre, F. (2010). Architecture and sedimentology of the Kerinitis Gilbert-type fan delta, Corinth Rift, Greece. *Sedimentology*, *57*(2), 543–586. https://doi.org/10.1111/j.1365-3091.2009.01105.x

Bagnold, R. A. (1941). *The physics of wind blown sand and desert dunes* (265 pp.). London: Methuen.

Bathurst, J. C. (1985). Flow resistance estimation in mountain rivers. *Journal of Hydraulic Engineering*, *111*(4), 625–643. https://doi.org/10.1061/(ASCE)0733-9429(1985)111:4(625)

Begin, Z. B., Meyer, D. F., & Schumm, S. A. (1981). Development of longitudinal profiles of alluvial channels in response to base-level lowering. *Earth Surface Processes and Landforms*, *6*(1), 49–68. https://doi.org/10.1002/esp. 3290060106

Blom, A., Chavarrías, V., Ferguson, R. I., & Viparelli, E. (2017). Advance, retreat, and halt of abrupt gravel-sand transitions in alluvial rivers. *Geophysical Research Letters*, *44*, 9751–9760. https://doi.org/10.1002/2017GL074231

Blom, A., & Kleinhans, M. G. (2006). Modelling sorting over the lee face of individual bed forms. In R. M. L. Ferreira (Ed.), *River Flow 2006: Proceedings of the International Conference on Fluvial Hydraulics* (pp. 807–816). Leiden, NL: Taylor and Francis.

Blom, A., & Parker, G. (2004). Vertical sorting and the morphodynamics of bed-form dominated rivers: A modeling framework. *Journal of Geophysical Research*, *109*, F02007. https://doi.org/10.1029/2003JF000069

Blom, A., Ribberink, J. S., & de Vriend, H. J. (2003). Vertical sorting in bed forms: Flume experiments with a natural and a trimodal sediment mixture. *Water Resources Research*, *39*(2), 1025. https://doi.org/10.1029/2001WR001088

Blom, A., Viparelli, E., & Chavarrías, V. (2016). The graded alluvial river: Profile concavity and downstream fining. *Geophysical Research Letters*, *43*, 6285–6293. https://doi.org/10.1002/2016GL068898

Boesch, D. F., Josselyn, M. N., Mehta, A. J., Morris, J. T., Nuttle, W., Simenstad, C. A., & Swift, D. J. P. (1994). Scientific assessment of coastal wetland loss, restoration and management in Louisiana. *Journal of Coastal Research: Special Issue*, *20*, 1–103.

Boyer, J., Duvail, C., Strat, P. L., Gensous, B., & Tesson, M. (2005). High resolution stratigraphy and evolution of the Rhône delta plain during Postglacial time, from subsurface drilling data bank. *Marine Geology*, *222-223*(Supplement C), 267–298. https://doi.org/10.1016/j.margeo.2005.06.017

Breda, A., Mellere, D., & Massari, F. (2007). Facies and processes in a Gilbert-delta-filled incised valley (Pliocene of Ventimiglia, NW Italy). *Sedimentary Geology*, *200*(1-2), 31–55. https://doi.org/10.1016/j.sedgeo.2007.02.008

Breda, A., Mellere, D., Massari, F., & Asioli, A. (2009). Vertically stacked Gilbert-type deltas of Ventimiglia (NW Italy): The Pliocene record of an overfilled Messinian incised valley. *Sedimentary Geology*, *219*, 58–76. https://doi.org/10.1016/j.sedgeo.2009.04.010

Brownlie, W. R. (1983). Flow depth in sand-bed channels. *Journal of Hydraulic Engineering*, *109*(7), 959–990. https://doi.org/10.1061/(ASCE)0733-9429(1983)109:7(959)

Chow, V. T. (1959). *Open-channel hydraulics* (680 pp.). New York: McGraw-Hill.

Culling, W. E. H. (1960). Analytical theory of erosion. *Journal of Geology*, *68*(3), 336–344. https://doi.org/10.1086/626663

Dabrio, C. J., Bardají, T., Zazo, C., & Goy, J. L. (1991). Effects of sea-level changes on a wave-worked Gilbert-type delta (Late Pliocene, Aguilas Basin, SE Spain). *Cuadernos de Geología Ibérica*, *15*, 103–137.

De Vries, M. (1973). River-bed variations-aggradation and degradation (Tech. Rep. 107). The Netherlands: Delft Hydraulics Laboratory.

De Vries, M. (1975). A morphological time-scale for rivers. In *Proceedings of the XVIth IAHR congress, São Paulo*.

Dietrich, W. E., Kirchner, J. W., Ikeda, H., & Iseya, F. (1989). Sediment supply and the development of the coarse surface layer in gravel-bedded rivers. *Nature*, *340*, 215–217. https://doi.org/10.1038/340215a0

Edmonds, D. A., Shaw, J. B., & Mohrig, D. (2011). Topset-dominated deltas: A new model for river delta stratigraphy. *Geology*, *39*(12), 1175–1178. https://doi.org/10.1130/G32358.1

Fasolato, G., Ronco, P., Langendoen, E. J., & Di Silvio, G. (2011). Validity of uniform flow hypothesis in one-dimensional morphodynamic models. *Journal of Hydraulic Engineering*, *137*(2), 183–195. https://doi.org/10.1061/(ASCE)HY.1943-7900.0000291

Ferguson, R. (2007). Flow resistance equations for gravel- and boulder-bed streams. *Water Resources Research*, *43*, W05427. https://doi.org/10.1029/2006WR005422

Ferrer-Boix, C., Martín-Vide, J. P., & Parker, G. (2015). Sorting of a sand-gravel mixture in a Gilbert-type delta. *Sedimentology*, *62*(5), 1446–1465. https://doi.org/10.1111/sed.12189

García-García, F., Fernández, J., Viseras, C., & Soria, J. (2006). High frequency cyclicity in a vertical alternation of Gilbert-type deltas and carbonate bioconstructions in the late Tortonian, Tabernas Basin, Southern Spain. *Sedimentary Geology*, *192*(3–4), 123–139. https://doi.org/10.1016/j.sedgeo.2006.03.025

Gilbert, G. K. (1877). *Report on the geology of the Henry Mountains* (160 pp.). Washington, DC: US Geographical and Geological Survey of the Rocky Mountain Region US Government Printing Office.

Gilbert, G. K. (1885). The topographic features of lake shores. *U.S. Geological Survey Annual Report*, *5*, 75–123.

Gilbert, G. K. (1890). Lake Bonneville, *US Geological Survey Monograph* (Vol. 1, 438 pp.). Washington, DC: US Government Printing Office.

Gilbert, G. K. (1914). The transportation of debris by running water, *US Geological Survey Professional Paper 86* (263 pp.). Washington, DC: US Government Printing Office.

Hirano, M. (1971). River bed degradation with armoring. *Proceedings of the Japan Society of Civil Engineers*, *195*, 55–65. https://doi.org/10.2208/jscej1969.1971.195_55

Hoey, T. B., & Ferguson, R. (1994). Numerical simulation of downstream fining by selective transport in gravel bed rivers: Model development and illustration. *Water Resources Research*, *30*(7), 2251–2260. https://doi.org/10.1029/94WR00556

Howard, A. (1980). Thresholds in river regimes. In D. R. Coates & J. D. Vitek (Eds.), *Thresholds in geomorphology* (pp. 227–258). Boston: George Allen and Unwin.

Howard, A. D. (1982). Equilibrium and time scales in geomorphology: Application to sand-bed alluvial streams. *Earth Surface Processes and Landforms*, *7*(4), 303–325. https://doi.org/10.1002/esp.3290070403

Kleinhans, M. G. (2005). Grain-size sorting in grainflows at the lee side of deltas. *Sedimentology*, *52*(2), 291–311. https://doi.org/10.1111/j.1365-3091.2005.00698.x

Kleinhans, M. G., van Dijk, W. M., van de Lageweg, W. I., Hoyal, D. C., Markies, H., van Maarseveen, M., et al. (2014). Quantifiable effectiveness of experimental scaling of river- and delta morphodynamics and stratigraphy. *Earth-Science Reviews*, *133*, 43–61. https://doi.org/10.1016/j.earscirev.2014.03.001

Kostic, S., & Parker, G. (2003a). Progradational sand-mud deltas in lakes and reservoirs. Part 1. Theory and numerical modeling. *Journal of Hydraulic Research*, *41*(2), 127–140. https://doi.org/10.1080/00221680309499956

Kostic, S., & Parker, G. (2003b). Progradational sand-mud deltas in lakes and reservoirs. Part 2. Experiment and numerical simulation. *Journal of Hydraulic Research*, *41*(2), 141–152. https://doi.org/10.1080/00221680309499957

Lai, S. Y. J., Hsiao, Y.-T., & Wu, F.-C. (2017). Asymmetric effects of subaerial and subaqueous basement slopes on self-similar morphology of prograding deltas. *Journal of Geophysical Research: Earth Surface*, *122*, 2506–2526. https://doi.org/10.1002/2017JF004244

Longhitano, S. G. (2008). Sedimentary facies and sequence stratigraphy of coarse-grained Gilbert-type deltas within the Pliocene thrust-top Potenza Basin (southern Apennines, Italy). *Sedimentary Geology*, *210*, 87–110. https://doi.org/10.1016/j.sedgeo.2008.07.004

Lorenzo-Trueba, J., Voller, V. R., Muto, T., Kim, W., Paola, C., & Swenson, J. B. (2009). A similarity solution for a dual moving boundary problem associated with a coastal-plain depositional system. *Journal of Fluid Mechanics*, *628*, 427–443. https://doi.org/10.1017/S0022112009006715

Mackin, J. H. (1948). Concept of the graded river. *Geological Society of America Bulletin*, *59*(5), 463–512. https://doi.org/10.1130/0016-7606(1948)59

Martín-Vide, J., Ferrer-Boix, C., & Ollero, A. (2010). Incision due to gravel mining: Modeling a case study from the Gállego River, Spain. *Geomorphology*, *117*(3), 261–271. https://doi.org/10.1016/j.geomorph.2009.01.019

Martini, I., Ambrosetti, E., & Sandrelli, F. (2017). The role of sediment supply in large-scale stratigraphic architecture of ancient Gilbert-type deltas (Pliocene Siena-Radicofani Basin, Italy). *Sedimentary Geology*, *350*, 23–41. https://doi.org/10.1016/j.sedgeo.2017.01.006

Meyer-Peter, E., & Müller, R. (1948). Formulas for bed-load transport. In *Proceedings of 2nd meeting of the International Association for Hydraulic Structures Research* (pp. 39–64). Stockholm.

Muto, T., & Steel, R. J. (1992). Retreat of the front in a prograding delta. *Geology*, *20*(11), 967–970. https://doi.org/10.1130/0091-7613(1992)020

Muto, T., & Swenson, J. B. (2005). Large-scale fluvial grade as a nonequilibrium state in linked depositional systems: Theory and experiment. *Journal of Geophysical Research*, *110*, F03002. https://doi.org/10.1029/2005JF000284

Nemec, W. (1990). Aspects of sediment movement on steep delta slopes, *Coarse-Grained Deltas* (pp. 29–73). Oxford, UK: Blackwell Ltd. https://doi.org/10.1002/9781444303858.ch3

Orrù, C., Blom, A., Chavarrías, V., Ferrara, V., & Stecca, G. (2016). A new technique for measuring the bed surface texture during flow and application to a degradational sand-gravel laboratory experiment. *Water Resources Research*, *52*, 7005–7022. https://doi.org/10.1002/2016WR018938

Orrù, C., Blom, A., & Uijttewaal, W. S. J. (2016). Armor breakup and reformation in a degradational laboratory experiment. *Earth Surface Dynamics*, *4*(2), 461–470. https://doi.org/10.5194/esurf-4-461-2016

Orrù, C., Chavarrías, V., Uijttewaal, W. S. J., & Blom, A. (2014). Image analysis for measuring the size stratification in sand-gravel laboratory experiments. *Earth Surface Dynamics*, *2*(1), 217–232. https://doi.org/10.5194/esurf-2-217-2014

Paola, C., Heller, P. L., & Angevine, C. L. (1992). The large-scale dynamics of grain-size variation in alluvial basins, 1: Theory. *Basin Research*, *4*(2), 73–90. https://doi.org/10.1111/j.1365-2117.1992.tb00145.x

Paola, C., & Mohrig, D. (1996). Palaeohydraulics revisited: Palaeoslope estimation in coarse-grained braided rivers. *Basin Research*, *8*(3), 243–254. https://doi.org/10.1046/j.1365-2117.1996.00253.x

Paola, C., Parker, G., Seal, R., Sinha, S. K., Southard, J. B., & Wilcock, P. R. (1992). Downstream fining by selective deposition in a laboratory flume. *Science*, *258*(5089), 1757–1760. https://doi.org/10.1126/science.258.5089.1757

Paola, C., Straub, K., Mohrig, D., & Reinhardt, L. (2009). The unreasonable effectiveness of stratigraphic and geomorphic experiments. *Earth-Science Reviews*, *97*(1-4), 1–43. https://doi.org/10.1016/j.earscirev.2009.05.003

Paola, C., Twilley, R. R., Edmonds, D. A., Kim, W., Mohrig, D., Parker, G., et al. (2011). Natural processes in delta restoration: Application to the Mississippi Delta. *Annual Review of Marine Science*, *3*(1), 67–91. https://doi.org/10.1146/annurev-marine-120709-142856

Parker, G. (1991a). Selective sorting and abrasion of river gravel. I: Theory. *Journal of Hydraulic Engineering*, *117*(2), 131–147. https://doi.org/10.1061/(ASCE)0733-9429(1991)117:2(131)

Parker, G. (1991b). Selective sorting and abrasion of river gravel. II: Applications. *Journal of Hydraulic Engineering*, *117*(2), 150–171. https://doi.org/10.1061/(ASCE)0733-9429(1991)117:2(150)

Parker, G., & Klingeman, P. C. (1982). On why gravel bed streams are paved. *Water Resources Research*, *18*(5), 1409–1423. https://doi.org/10.1029/WR018i005p01409

Parker, G., Muto, T., Akamatsu, Y., Dietrich, W. E., & Lauer, J. W. (2008). Unravelling the conundrum of river response to rising sea-level from laboratory to field. Part I: Laboratory experiments. *Sedimentology*, *55*(6), 1643–1655. https://doi.org/10.1111/j.1365-3091.2008.00961.x

Parker, G., & Sutherland, A. J. (1990). Fluvial armor. *Journal of Hydraulic Research*, *28*(5), 529–544. https://doi.org/10.1080/00221689009499044

Posamentier, H. W., & Allen, G. P. (1993). Variability of the sequence stratigraphic model: Effects of local basin factors. *Sedimentary Geology*, *86*(1), 91–109.

Posamentier, H. W., Allen, G. P., James, D. P., & Tesson, M. (1992). Forced regressions in a sequence stratigraphic framework: Concepts, examples, and exploration significance. *American Association of Petroleum Geologists Bulletin*, *76*(11), 1687–1709.

Postma, G. (1990). An analysis of the variation in delta architecture. *Terra Nova*, *2*, 124–130. https://doi.org/10.1111/j.1365-3121.1990.tb00052.x

Postma, G. (1995). Sea-level-related architectural trends in coarse-grained delta complexes. *Sedimentary Geology*, *98*, 3–12. https://doi.org/10.1016/0037-0738(95)00024-3

Recking, A., Frey, P., Paquier, A., & Belleudy, P. (2009). An experimental investigation of mechanisms involved in bed load sheet production and migration. *Journal of Geophysical Research*, *114*, F03010. https://doi.org/10.1029/2008JF000990

Ribberink, J. S., & Van der Sande, J. T. M. (1985). Aggradation in rivers due to overloading-analytical approaches. *Journal of Hydraulic Research*, *23*(3), 273–283. https://doi.org/10.1080/00221688509499355

Ronco, P., Fasolato, G., Nones, M., & Di Silvio, G. (2010). Morphological effects of damming on lower Zambezi River. *Geomorphology*, *115*(1), 43–55. https://doi.org/10.1016/j.geomorph.2009.09.029

Seminara, G., Colombini, M., & Parker, G. (1996). Nearly pure sorting waves and formation of bedload sheets. *Journal of Fluid Mechanics*, *312*, 253–278. https://doi.org/10.1017/S0022112096001991

Simons, D. B., Richardson, E. V., & Nordin, C. F. (1965). Bedload equation for ripples and dunes. In *US Geological Survey Professional Paper 462-H* (p. 9). Washington, DC: US Government Printing Office.
Smith, D. G., & Jol, H. M. (1997). Radar structure of a Gilbert-type delta, Peyto Lake, Banff National Park, Canada. *Sedimentary Geology*, *113*(3–4), 195–209. https://doi.org/10.1016/S0037-0738(97)00061-4
Snow, R. S., & Slingerland, R. L. (1987). Mathematical modeling of graded river profiles. *Journal of Geology*, *95*(1), 15–33.
Sternberg, H. (1875). Untersuchungen über Längen- und Querprofil geschiebeführender Flüsse (in German). *Zeitschrift für Bauwesen*, *25*, 483–506.
Swenson, J. B., & Muto, T. (2007). Response of coastal plain rivers to falling relative sea-level: Allogenic controls on the aggradational phase. *Sedimentology*, *54*(1), 207–221. https://doi.org/10.1111/j.1365-3091.2006.00830.x
Swenson, J. B., Voller, V. R., Paola, C., Parker, G., & Marr, J. (2000). Fluvio-deltaic sedimentation: A generalized Stefan problem. *European Journal of Applied Mathematics*, *11*(05), 433–452. https://doi.org/10.1017/S0956792500004198
Thompson, S. M., & Campbell, P. L. (1979). Hydraulics of a large channel paved with boulders. *Journal of Hydraulic Research*, *17*(4), 341–354. https://doi.org/10.1080/00221687909499577
Toro-Escobar, C. M., Paola, C., & Parker, G. (1996). Transfer function for the deposition of poorly sorted gravel in response to streambed aggradation. *Journal of Hydraulic Research*, *34*(1), 35–53. https://doi.org/10.1080/00221689609498763
Van Bendegom, L. (1947). Eenige beschouwingen over riviermorphofogie en rivierverbetering (in Dutch). *De Ingenieur*, *59*(4), 1–11.
Vanoni, V. A., & Brooks, N. H. (1957). Laboratory studies of the roughness and suspended load of alluvial streams (Sedimentation Laboratory Report E-68) (121 pp.). Pasadena, CA: California Institute of Technology.
Viparelli, E., Blom, A., Ferrer-Boix, C., & Kuprenas, R. (2014). Comparison between experimental and numerical stratigraphy emplaced by a prograding delta. *Earth Surface Dynamics*, *2*(1), 323–338. https://doi.org/10.5194/esurf-2-323-2014
Viparelli, E., Blom, A., & Parker, G. (2012). Modeling stratigraphy formed by prograding Gilbert-type deltas. In Murillo-Muñoz (Ed.), *River Flow 2012: Proceedings of the International Conference on Fluvial Hydraulics* (pp. 5–7). London: CRC Press, Taylor and Francis Group.
Viparelli, E., Haydel, R., Salvaro, M., Wilcock, P. R., & Parker, G. (2010). River morphodynamics with creation/consumption of grain size stratigraphy 1: Laboratory experiments. *Journal of Hydraulic Research*, *48*(6), 715–726. https://doi.org/10.1080/00221686.2010.515383
Whiting, P. J., Dietrich, W. E., Leopold, L. B., Drake, T. G., & Shreve, R. L. (1988). Bedload sheets in heterogeneous sediment. *Geology*, *16*(2), 105–108. https://doi.org/10.1130/0091-7613(1988)016<0105:BSIHS>2.3.CO;2
Wilcock, P. R., & Crowe, J. C. (2003). Surface-based transport model for mixed-size sediment. *Journal of Hydraulic Engineering*, *129*(2), 120–128. https://doi.org/10.1061/(ASCE)0733-9429(2003)129:2(120)
Wright, S., & Parker, G. (2005a). Modeling downstream fining in sand-bed rivers. I: Formulation. *Journal of Hydraulic Research*, *43*(6), 613–620. https://doi.org/10.1080/00221680509500381
Wright, S., & Parker, G. (2005b). Modeling downstream fining in sand-bed rivers. II: Application. *Journal of Hydraulic Research*, *43*(6), 621–631. https://doi.org/10.1080/00221680509500382